

Anti-angiogenic and pro-apoptotic effects of a small-molecule JFD-WS in *in vitro* and breast cancer xenograft mouse models

APPU RATHINAVELU, THANIGAIVELAN KANAGASABAI,
SIVANESAN DHANDAYUTHAPANI and KHALID ALHAZZANI

Rumbaugh-Goodwin Institute for Cancer Research, College of Pharmacy, Health Professions Division,
Nova Southeastern University, Fort Lauderdale, FL 33328, USA

Received May 15, 2017; Accepted October 26, 2017

DOI: 10.3892/or.2018.6256

Abstract. A small molecule that was developed for blocking vascular endothelial growth factor receptor 2 (VEGFR2) has been tested and confirmed for its anti-angiogenic activity. Subsequently, it was modified into a water soluble salt form (JFD-WS) to increase bioavailability and distribution during *in vivo* pre-clinical testing. The present study was designed to further evaluate the anti-angiogenic and pro-apoptotic effects of JFD-WS in monotherapy as well as in combination with paclitaxel (Taxol) using a mouse xenograft model. The *in vitro* anti-angiogenic effects of JFD-WS were investigated using cell proliferation, migration, Matrigel tube formation and VEGFR2 phosphorylation assays. The anti-angiogenic effect of JFD-WS was further established using chorioallantoic membrane (CAM) assay followed by *in vivo* efficacy testing on GI-101A breast adenocarcinoma cells. Pharmacokinetic and toxicity studies were performed using BALB/c mice. Finally, the apoptotic signals were assessed in the control and experimental tumor samples, and the plasma mucin 1 (MUC1) levels were analyzed. In the *in vitro* tests, JFD-WS effectively inhibited HUVEC proliferation, migration, tube formation and VEGFR2 phosphorylation. Additionally, JFD-WS inhibited the formation of blood vessels in chick chorioallantoic membrane. While inhibiting the xenograft tumor growth in experimental mice, JFD-WS decreased the plasma MUC1 levels. The western blot analysis of apoptotic markers and fragmentation analysis of DNA confirmed the pro-apoptotic effects of JFD-WS. These results indicated that JFD-WS alone or in combination with paclitaxel exerted antitumor and pro-apoptotic effects in the breast cancer xenograft model due to an anti-angiogenic effect. These results strongly support the clinical translation of its use.

Introduction

The growth of solid tumors, as well as the metastasis of aggressive cancers, depend on angiogenesis and lymphangiogenesis that are triggered by chemical signals originating from the tumor cells during the phase of rapid growth (1). Generally angiogenesis, the process of new blood vessel formation, is inactive in normal vasculature except during the wound healing process, where angiogenesis is transiently turned on in order to facilitate the healing of wound tissue. However, it plays a central role in regulating local tumor growth, invasion and distant metastasis of various cancers including breast cancers (2). Among the known pro-angiogenic factors, the dominant regulator of normal and pathological angiogenesis is vascular endothelial growth factor (VEGF) and its receptors (VEGFRs). Activation of the VEGFR2 signaling pathway leads to phosphorylation of various downstream signal transduction proteins, including phosphoinositide 3-kinase and protein kinase B (PI3K-AKT), p38 mitogen-activated protein kinase (p38 MAPK), and extracellular signal-regulated kinase (ERK), to promote the pro-angiogenic effects, which include endothelial cell proliferation, migration and tube formation resulting in the creation of new vascular walls. Therefore, antagonizing VEGFR2 has become one of the common modes of cancer therapy for its role in inhibiting tumor growth and metastasis (3). However, current cancer therapies are often discontinued due to considerable side-effects (4). Therefore, it is necessary to search for new drugs that have the ability to attack specific tumor targets to arrest growth or sensitize cancer cells to cytotoxic chemotherapy to enhance therapeutic outcomes (4).

In this context, a novel small molecule code named JFD was developed using molecular modeling (MODELLER 6v2) to specifically antagonize VEGFR2 (5). The model was refined further by energy minimization using DISCOVER module of Insight II Accelrys Inc. (San Diego, CA, USA) (5). The JFD original with poor water solubility was modified into a water soluble form (JFD-WS) to enhance the bioavailability. Prior to the development of JFD-WS, the parent compound JFD original was tested and confirmed for its anti-angiogenic activity using HUVEC Matrigel assay (5,6). Several *in vitro* studies have attempted to recreate the complex sequence of angiogenic events using HUVEC cells. Therefore, HUVECs

Correspondence to: Dr Appu Rathinavelu, Rumbaugh-Goodwin Institute for Cancer Research, College of Pharmacy, Health Professions Division, Nova Southeastern University, 3321 South University Drive, Fort Lauderdale, FL 33328, USA
E-mail: appu@nova.edu

Key words: anti-angiogenesis, apoptosis, breast cancer, JFD-WS, GI-101A cells

are used as the cell based (*in vitro*) model to study abnormal and tumor-associated angiogenesis (7). In addition to confirmation of the anti-angiogenic properties, both the JFD original and JFD-WS were shown to have antitumorogenic effects in a patient-derived xenograft (PDX) implanted animal model (6). As seen with several anti-angiogenic drugs, JFD-WS produces significant control of cancer growth when used in combination with paclitaxel (Taxol). The cytotoxic compound paclitaxel is classified as a taxane, an anti-microtubule agent with a unique mechanism of action and potent cytotoxic activity against several tumor types, including ovarian, breast, lung and bladder (8,9). Taxol inhibits the cell cycle at the G2-M phase transition points and subsequently induces apoptosis of cancer cells (10). The two most commonly described pathways of apoptosis are the death receptor-mediated (extrinsic) and the mitochondria-mediated (intrinsic) pathway. The extrinsic pathway is initiated by activation of death receptors of the tumor necrosis factor (TNF) superfamily that are expressed on the cell surface. The intrinsic pathway is typically initiated subsequent to chemotherapy treatment, growth factor withdrawal, hypoxia or via induction of tumor-suppressor genes (11). Apart from evaluating the pro-apoptotic signals, we also assessed the tumor burden by measuring the levels of circulating tumor marker MUC1 (CA 15-3), a transmembrane glycoprotein of the mucin family, which is overexpressed in >90% of breast carcinomas (12). Due to overexpression and its secretion into the blood circulation, MUC1 is considered as a tumor marker (13).

Therefore, the main focus of the present study was to determine the anti-angiogenic and pro-apoptotic effects of JFD-WS alone and in combination with Taxol in GI-101A xenografts, a PDX breast cancer mouse model. In addition, the chronic toxicity of JFD-WS alone and in combination with Taxol was also studied. Taken together, our data suggest that JFD-WS could be further advanced towards the clinical translation of its use.

Materials and methods

Cell lines and reagents. For *in vitro* experiments, HUVECs were purchased from Lonza (Walkersville, MD, USA) and maintained in endothelial cell growth medium-2 (EGM-2) supplemented with BulletKit containing VEGF and all the required growth factors. Cells were incubated at 37°C in a humidified incubator with 95% air, 5% CO₂. For *in vivo* experiments, GI-101A human breast carcinoma cells derived at the Rumbaugh-Goodwin Institute for Cancer Research (Plantation, FL, USA) from a 57-year-old female patient with recurrent ductal adenocarcinoma (stage IIIa; T3N2MX) who had not previously received any chemotherapy or radiation therapy other than surgery were used in the present study (14). GI-101A and MCF-7 cells were maintained in RPMI-1640 and Dulbecco's modified Eagle's medium (DMEM), respectively, supplemented with 10% fetal bovine serum (FBS), 2 mM L-glutamine, 1.5 g/l sodium bicarbonate and 1% penicillin/streptomycin. Cultures were incubated under the same aforementioned conditions. Only single-cell suspensions with >95% viability were used for injection into the experimental mice. The antibodies against p53 (9282; 1:1,000 rabbit polyclonal), Bcl-2 (D55G8; 1:1,000 rabbit monoclonal),

Bax (D2E11; 1:1,000 rabbit monoclonal), APAF-1 (D7G4; 1:1,000 rabbit monoclonal), cytochrome *c* (D18C7; 1:1,000 rabbit monoclonal), PARP (46D11; 1:1,000 rabbit monoclonal), phospho-VEGFR2 (19A10; 1:1,000 rabbit monoclonal) and cleaved caspase-3 (9662; 1:1,000 rabbit polyclonal) were purchased from Cell Signaling Technology (Danvers, MA, USA). Sunitinib was purchased from Sigma-Aldrich Co. (St. Louis, MO, USA). All other chemicals used in this experiment were of research grade.

Cell proliferation assay. The proliferation of HUVECs was determined by bromodeoxyuridine (BrdU) labeling assay. Briefly, HUVECs were plated at 5x10³ cells/well in 96-well plates and allowed to attach for 24 h in EGM-2 BulletKit (100 µl/well). Cells were exposed to different concentrations of JFD-WS (1-40 µM) and incubated in the presence of 1X BrdU for 24 h, and then assayed with BrdU Cell Proliferation kit (Cell Signaling Technology) following the manufacturer's instructions.

Cytotoxicity assay using MCF-7 and GI-101A cells. To further confirm the effect of JFD-WS on breast cancer cell lines, cytotoxicity on GI-101A and MCF-7 cells was assessed using trypan blue dye exclusion method. Briefly, the cells were treated with different concentrations of JFD-WS (1-100 µM) for 24 h. Then, the cell death was determined by calculating the relative percentage of live cells.

Cell migration assay. The effect of JFD-WS on cell migration was assessed using both Transwell and scratch assays. For Transwell migration assay, 6.5-mm Transwell inserts with an 8-µm polycarbonate membrane (Corning Inc., Corning, NY, USA) were used. The upper chamber of the Transwell contained HUVECs suspended with basal media exposed to different concentrations of JFD-WS. The lower chamber was filled with EGM-2 supplemented with 50 ng/ml VEGF-A as a chemoattractant. Then, the Transwell plates were incubated for 24 h to allow for migration of HUVECs across the porous membrane. Transwell filters were fixed in 70% ethanol and stained with crystal violet and examined under a Leica microscope (DMI3000 B; Leica Microsystems, Inc., Buffalo, Grove, IL, USA). Migratory cells were detached from the lower chamber and counted using Bio-Rad TC10™ automated cell counter. For the scratch assay, a confluent monolayer of HUVECs was grown on 24-well plates. A sterile 200-µl tip was used to scratch a straight line and fresh medium with corresponding concentrations of JFD-WS (0.1-10 µM) was added to the scratched monolayer. The drug concentrations used in this assay were determined based on the results obtained from the Transwell migration assay, in which we observed >70% inhibition at 10 µM. Therefore, 10 µM JFD-WS was used as a maximum concentration for the scratch assay. Images were captured using Leica microscope (DMI3000 B) at 12 h post-scratch. The cell migratory effect of JFD-WS was calculated as the percentage of the cell migration after 12 h. Images were analyzed using ImageJ software (<http://rsbweb.nih.gov/ij/download.html>).

Matrigel tube formation assay. The anti-angiogenesis ability of JFD-WS was evaluated using the Chemicon *in vitro*

angiogenesis assay kit (ECM 625; Millipore, Billerica, MA, USA). Briefly, a 96-well plate was pre-incubated with EC-Matrigel at 37°C for 1 h. Then, HUVECs (1x10⁴ cells) suspended in the EGM-2 medium were seeded onto the Matrigel and treated with various concentrations of JFD-WS (0.05-10 μM). After a 6-h incubation at 37°C, tube formation was assessed by counting the capillary tube branch points in 5 randomly selected fields for each well using Leica microscope (DMI3000 B). The capillary network formation was scored according to the method of Sridhar *et al* (5). Sunitinib was used as a positive control.

Inhibition of growth factor-stimulated VEGFR2 phosphorylation in vitro. The ability of JFD-WS to inhibit VEGFR2 phosphorylation was determined using western blotting. HUVECs were treated with JFD-WS (2 μM) in the presence and absence of VEGF (50 ng/ml). After 24 h of treatment, the cells were lysed on ice; proteins were extracted and analyzed by western blotting. Protein sample extracted from sunitinib-treated cells was included as a positive control.

Phospho-VEGFR2 sandwich ELISA assay. Endogenous levels of phospho-VEGFR2 (Tyr1175) were determined using PathScan[®] Phospho-VEGFR2 (Tyr1175) Sandwich ELISA kit (Cell Signaling Technology). Briefly, the protein samples were diluted to the equal concentration; 100 μl of each diluted cell lysate was added to the mouse anti-VEGFR2 antibody-coated microwells and allowed to incubate overnight. Then, the microwells were incubated with rabbit anti-pVEGFR2 (Y1175) detection antibody followed by horseradish peroxidase (HRP)-linked secondary antibody and then developed with 3,3',5,5'-tetramethylbenzidine (TMB) substrate. Absorbance was read at 450 nm after adding the stop solution, and the results were recorded using a VersaMax microplate reader (Molecular Devices, Sunnyvale, CA, USA). Sunitinib was used as a positive control.

Chorioallantoic membrane (CAM) angiogenesis assay. The CAM assay was performed according to the method described by Tamilarasan *et al* (15). Fertilized chicken eggs were incubated in an automated digital egg incubator at 37°C and 67% relative humidity (RH). On the fourth day, the incubated eggs were broken and gently plated on Petri dishes under sterile conditions. JFD-WS at 5 and 10 μM concentrations was added to a paper disc containing 50 ng/ml VEGF and incubated for 12 and 24 h. Images were captured using a digital camera (Canon PowerShot A810). Angiogenesis was quantified by counting the number of branching blood vessels.

Treatment with PDX-implanted athymic nude mice. Eight- to 10-week-old in-house bred female athymic nude mice, weighing ~25 g, were used for tumor implantation. All animal care and experiments were performed in accordance with the guidelines and approval of the Institutional Animal Care and Use Committee (IACUC) of Nova Southeastern University. Briefly, 3.0x10⁶ cells were subcutaneously injected into the right flank of athymic nude mice. The tumor-bearing mice were divided randomly into 4 groups: group I was the untreated control; group II was treated with JFD-WS (100 mg/kg); group III was treated with Taxol (10 mg/kg); and group IV

was treated with the combination of JFD-WS (100 mg/kg) and Taxol (10 mg/kg). The experimental mice were treated once every 2 days for a period of 22 days. The tumor volume (V) was calculated according to the formula: $V = \frac{1}{2} \times (L \times W^2)$ where L, is the length and W, is the width. All the animals in the control and experimental groups were sacrificed at the end of the treatment. Blood samples were collected and plasma was separated for MUC1 analysis. The tumor tissues from control and experimental animals were harvested for DNA isolation and protein extraction.

Plasma MUC1 levels. Enzyme-linked immunosorbent assay (ELISA) was used for measuring the levels of MUC1 following the manufacturer protocol (Sigma-Aldrich, St. Louis, MO, USA). Briefly, the plasma collected from the control and experimental animals was added to microwells coated with anti-MUC1 antibody and allowed to incubate for 2 h at 37°C. Then, the microwells were incubated with rabbit anti-MUC1 detection antibody followed by HRP-conjugated secondary antibody. The color for the measurement was developed using TMB substrate. The absorbance was read at 450 nm after adding the stop solution, and the results were recorded using a microplate reader (Molecular Devices).

Western blot analysis. Tumor tissues (50 mg) were homogenized, and the tissue lysates were subjected to western blot analysis. Briefly, 25 μg of total protein was subjected to electrophoresis on 10-12% polyacrylamide gel, and then transferred onto a nitrocellulose membrane. After blocking with 5% non-fat dry milk solution, the membranes were probed with antibodies for p53, Bcl-2, Bax, APAF-1, PARP, cytochrome *c* and cleaved caspase-3 (1:1,000 dilution). The protein bands were visualized using the LumiGLO chemiluminescence substrate system (KPL Biosolutions, Milford, MA, USA) after incubation of the blotted membrane with HRP-conjugated secondary antibody (anti-rabbit A6154; 1:10,000; Sigma, St. Louis, MO, USA). As a loading control, membranes were stripped and reprobed with β-actin (A5441; 1:5,000 dilution; Sigma). The protein band intensity was quantified using ImageJ software (<http://rsbweb.nih.gov/ij/download.html>).

DNA fragmentation assay. DNA fragmentation was determined by gel electrophoresis. For this experiment, tumor tissue (~25 mg) was collected to extract DNA using DNeasy[®] Blood and Tissue kit (Qiagen, Valencia, CA, USA). DNA extracts (50 ng) mixed with peqGreen were loaded onto a 1.5% agarose gel, and then electrophoresis was performed at 50 V for 2 h. The gel also contained a DNA ladder for comparing the sizes of the DNA fragments.

Evaluation of chronic toxicity with JFD-WS. To test the potential toxicity of JFD-WS, 8- to 10-week-old in-house bred BALB/c mice (weight, 22-30 g) were used. All animals were maintained under sterile 12 h light-dark controlled conditions. They also had free access to autoclaved water and a conventional mouse diet throughout the experiment. The experimental animals were divided into 4 groups (6 in each group). The first group was the control that was not treated with any drug; the second group was injected with JFD-WS (100 mg/kg body weight); the third group was injected with Taxol (10 mg/kg

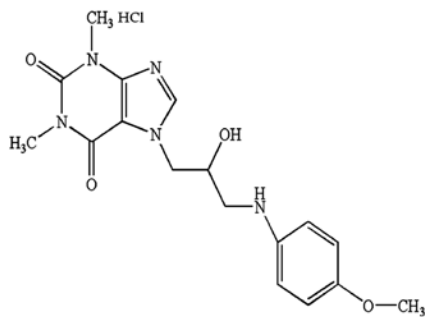


Figure 1. Chemical structure of JFD-WS. JFD-WS has a molecular formula $C_{16}H_{16}O_2$ with a molecular weight of 395.84 g/mol.

body weight) and the fourth group was injected with JFD-WS (100 mg/kg body weight) and Taxol (10 mg/kg body weight). The injections were given intraperitoneally (i.p.) once every 2 days for the duration of 30 days. All the animals were monitored twice a day for harmful side-effects such as allergy or ulceration, anorexia, and other relevant symptoms. At the end of the treatment period, blood samples were collected for performing blood chemistry and hematological analysis.

Pharmacokinetic studies. All pharmacokinetic parameters were evaluated using BALB/c mice. Briefly, JFD-WS was dissolved in sterile water and given i.p. at a concentration of 100 mg/kg body weight. The plasma samples (100 μ l) were collected at different time points (2.5-1,440 min) while 20 μ l urine samples were collected at 15-1,440 min. Then, JFD-WS

was extracted using simple liquid extraction procedure with HPLC grade acetonitrile (ACN). Final extracts were analyzed by reverse-phase high-performance liquid chromatography (Hitachi 2000, Monroe, GA, USA). The stationary phase consisted of Hitachi Lachrom C18 column (15 x 4.6 mm; 5 μ m particle size), whereas the mobile phase consisted of 100% ACN.

Statistical analysis. The data presented in the present study represent mean \pm standard deviation (SD) values from at least 4 independent experiments. Statistical analyses were performed using a one-way analysis of variance (ANOVA) and the differences between means were tested by unpaired Student's t-test using SPSS software (SPSS, Inc., Chicago, IL, USA). The value of $P < 0.05$ was considered as statistically significant.

Results

Effect of JFD-WS on HUVEC proliferation and migration. JFD-WS was designed to be easily dissolved in aqueous solutions. Its chemical structure is shown in Fig. 1. We initially sought to confirm the inhibitory effects of JFD-WS on endothelial cell (EC) proliferation. As shown in Fig. 2A, the proliferation of HUVECs stimulated by VEGF was significantly decreased after JFD-WS treatment at a concentration ranging from 5 to 40 μ M. In contrast, trypan blue assay results exhibited significant dose-dependent cell viability reduction of MCF-7 and GI-101A cells with IC_{50}

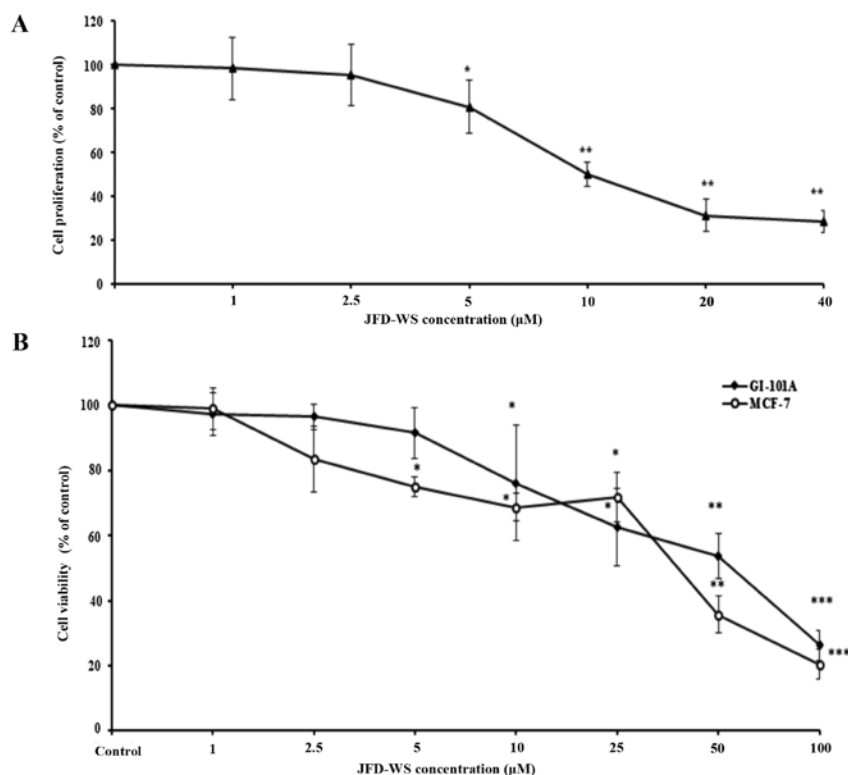


Figure 2. (A) JFD-WS inhibits VEGF-stimulated endothelial cell proliferation. HUVECs were treated with JFD-WS (1-40 μ M) for 24 h. Proliferation was then assessed by BrdU assay. Data represent mean \pm SD of 3 independent experiments. Significance was tested using a two-tailed t-test compared to the untreated cells (* $P \leq 0.05$, ** $P \leq 0.01$). (B) The effect of JFD-WS on breast cancer cell viability. GI-101A and MCF-7 breast cancer cells were treated with different doses of JFD-WS for 24 h. Trypan blue assay showed a dose-dependent decrease in cell viability in MCF-7 and GI-101A cells compared to the control group (untreated cells). Here, the control group is referred as 100% of viable cells. Data represent mean \pm SD of 3 independent experiments (* $P \leq 0.05$, ** $P \leq 0.01$, *** $P \leq 0.005$).

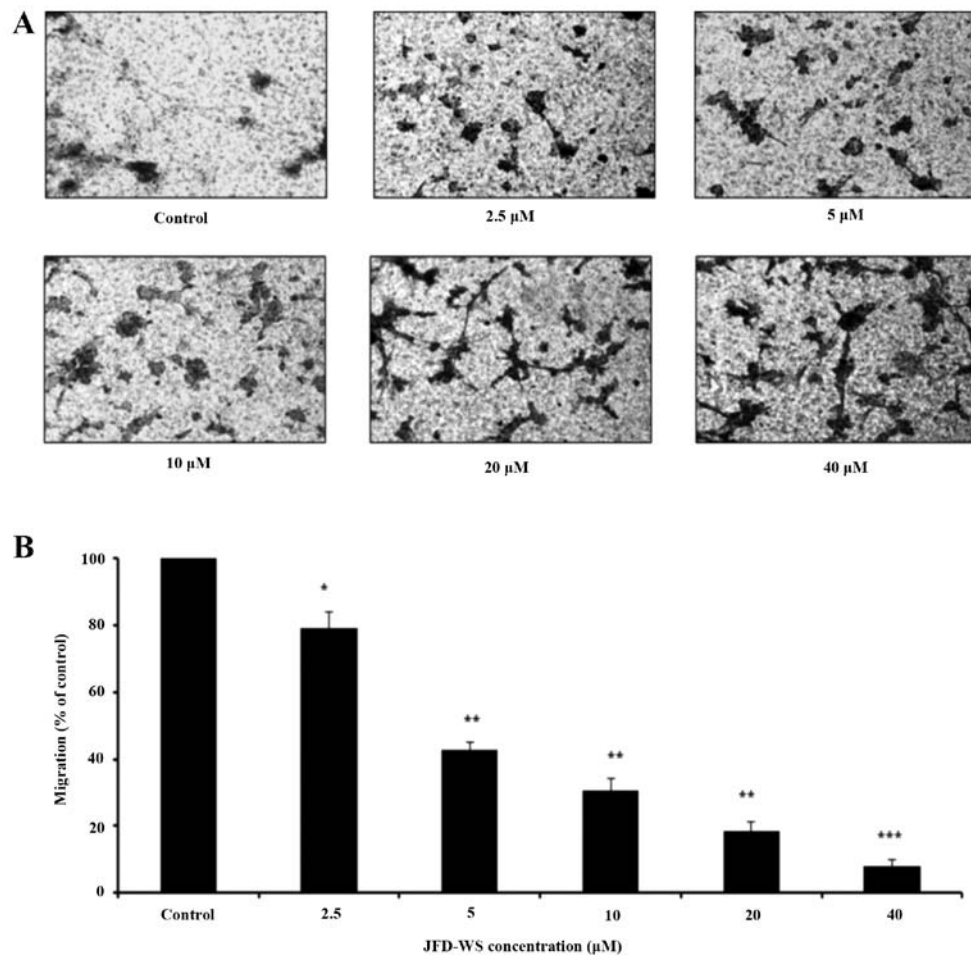


Figure 3. Effect of JFD-WS on the migratory potential of HUVECs was analyzed using *in vitro* Transwell assay. (A) Representative images depicting migration by HUVECs following exposure to JFD-WS. After 12 h of incubation, the cells remaining on the porous membrane (inserts) were fixed in 70% ethanol and stained with crystal violet and examined under Leica microscope. (B) Migrated cells on the lower chamber in the control and treatment groups were counted using TC10 automated cell counter. Data represent quantification of the percentage of migration in the treatment groups with respect to the control (* $P \leq 0.05$, ** $P \leq 0.01$, *** $P \leq 0.005$).

values of 36.5 and 55.5 μM respectively, after a 24-h treatment with JFD-WS (Fig. 2B). To further confirm the anti-angiogenic property of JFD-WS, we explored the effect of JFD-WS on the migration of HUVECs using Transwell migration assay. Our results showed that JFD-WS significantly inhibited the migration ability of HUVECs in a concentration-dependent manner (Fig. 3A), which is well correlated with the fewer number of migrated JFD-WS-treated cells in the lower chamber (Fig. 3B). After 24 h, ~90% of HUVECs were trapped in the upper compartment when treated with 40 μM JFD-WS as compared to the untreated cells, indicating a potential anti-migratory effect of JFD-WS (Fig. 3A). Similarly, JFD-WS exhibited consistent inhibitory effects on cell migration when assayed by scratch assay (Fig. 4A and B).

Inhibition of HUVEC tube formation and VEGFR2 phosphorylation. Beyond endothelial cell proliferation and migration, angiogenesis is dependent on the ability of ECs to organize and form cellular networks. Therefore, the ability of JFD-WS to inhibit angiogenesis was evaluated using capillary tube formation assay. As shown in Fig. 5A, HUVECs were seeded on Matrigel and treated with increasing concentrations of JFD-WS. Untreated HUVECs formed capillary-like

structures within 6 h. However, JFD-WS strongly inhibited the tube formation of HUVECs in a concentration-dependent manner (0.05-10 μM). Almost the maximum destruction of tube network was observed when HUVECs were incubated with JFD-WS at 10 μM . Then, we investigated the effects of JFD-WS on phospho-VEGFR2 protein expression. As shown in Fig. 5B, there was a significant reduction in VEGF-stimulated phospho-VEGFR2 levels in HUVECs treated with JFD-WS at a 2 μM concentration. In addition, the effect of JFD-WS on VEGF-induced tyrosine phosphorylation activity of VEGFR2 was measured using PathScan Sandwich ELISA kit. Results in Fig. 5C, show that the phosphorylation activity of VEGFR2 was increased by the exogenously added VEGF. However, the VEGF-induced phosphorylation activity of VEGFR2 was significantly attenuated in cells treated with JFD-WS.

Effects of JFD-WS on angiogenesis using CAM. To confirm the anti-angiogenic effects of JFD-WS, CAM assay was performed with 5 and 10 μM concentrations of JFD-WS. The number of blood vessels formed in the chorioallantoic membrane was significantly suppressed in both 5 and 10 μM JFD-WS treated groups as compared with the controls (Fig. 6A). The number of newly formed vessels was suppressed by ~40% ($P < 0.01$) and

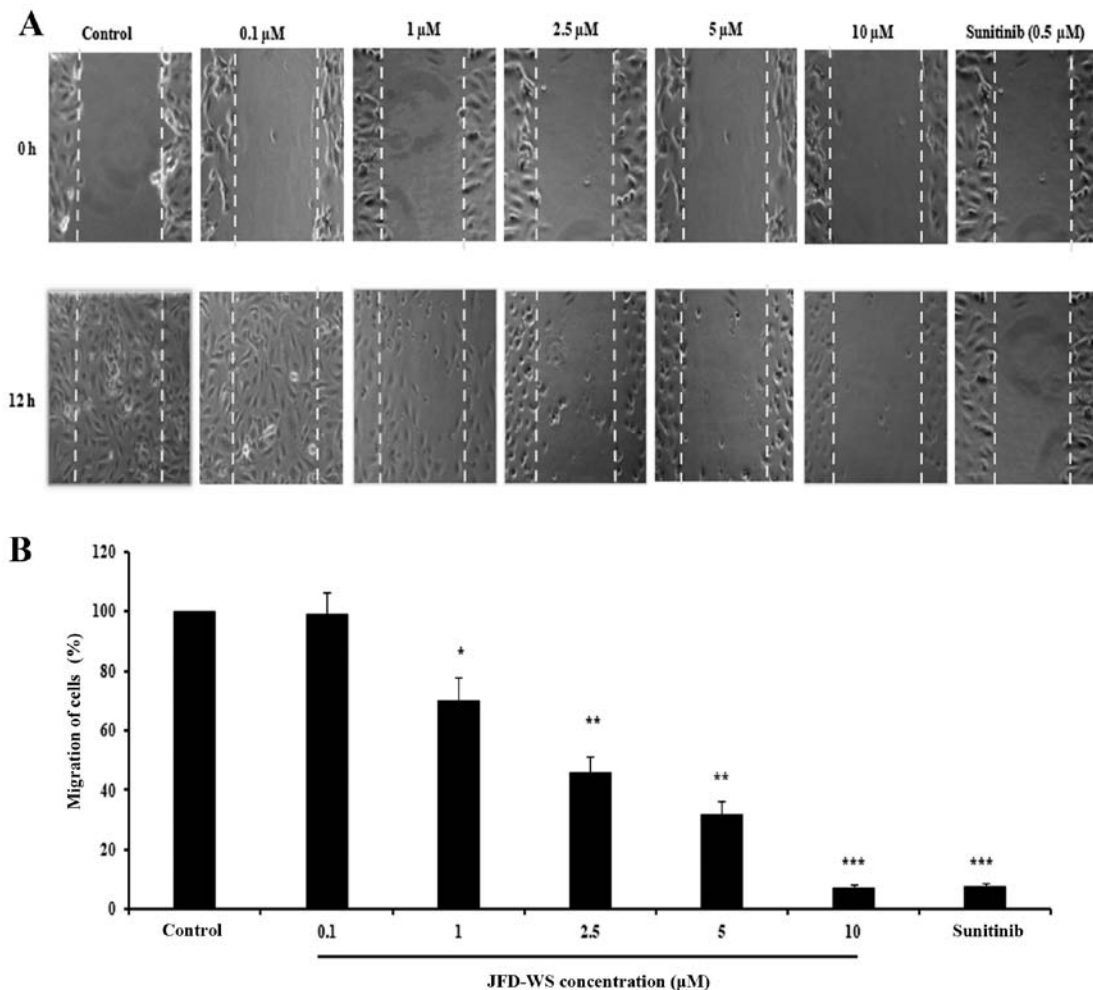


Figure 4. Inhibitory effects of JFD-WS on cell migration using scratch assay. (A) Representative images of endothelial cell migration with different concentrations of JFD-WS after 12 h of incubation. (B) Quantification of the percentage of migration in the treatment groups with respect to the control. Sunitinib (0.5 μ M) was used as a positive control (* P ≤0.05, ** P ≤0.01, *** P ≤0.005).

70% (P <0.001) after 12 and 24 h treatment of 5 μ M JFD-WS, respectively. However, the inhibition of blood vessel formation by JFD-WS was significantly higher at 10 μ M after 12 h (70%; P <0.001) and 24 h (94%; P <0.001) compared to lower concentrations (Fig. 6B).

Antitumor efficacy of JFD-WS in a GI-101A breast xenograft mouse model. The effect of JFD-WS on growth and metastasis of breast cancer was examined using immunocompromised nude mice implanted with GI-101A breast xenografts. To assess the effectiveness of JFD-WS, tumor volume and body weight of tumor-bearing animals were observed every 3 days until the end of the experiment. Mice implanted with GI-101A tumors showed 40 and 50% suppression of tumor growth after treatment with 100 mg/kg JFD-WS and 10 mg/kg Taxol, respectively, for 22 days (Fig. 7A-E). The doses of JFD-WS used in the present study were based on our initial experiments in which, we used 50 mg/kg body weight (data not shown) and 100 mg/kg body weight JFD-WS. However, better pharmacological (Fig. 7A-E) effects were observed in animals treated with 100 mg/kg body weight JFD-WS. Notably, the inhibitory effect of JFD-WS monotherapy was comparable to Taxol at the specified dose with no signs of toxicity. In contrast, 100 mg/kg dose of Taxol produced >50% mortality in the experimental

groups (data not shown). However, JFD-WS combination with Taxol treatment caused 85% suppression of tumor growth (Fig. 7D and E) confirming the additive effects of JFD-WS with no observed toxicity symptoms. Thus, JFD-WS combination with Taxol was well-tolerated, and there were no significant changes in food intake or body weight during the experimental period (Fig. 7F).

Effect of JFD-WS on plasma MUC1 levels. Since MUC1 is currently used as a marker of responsive therapy and as a prognostic indicator for survival, the effect of JFD-WS on the plasma levels of MUC1 in control mice with no tumor burden and tumor-bearing mice with and without treatment were analyzed using ELISA. As shown in Fig. 8, the level of MUC1 in tumor-bearing animals was nearly 80% higher when compared to the control animals. However, the level of MUC1 in JFD-WS and Taxol-treated animals showed 50 and 60% decrease respectively, after 22 days of treatment. Notably, an additional 9% decrease was observed when JFD-WS was treated in combination with Taxol. The effect of the combination treatment was found to be higher than the individual drug treatments.

JFD-WS increases p53 protein expression. To determine whether induction of apoptosis is preceded by activation of the

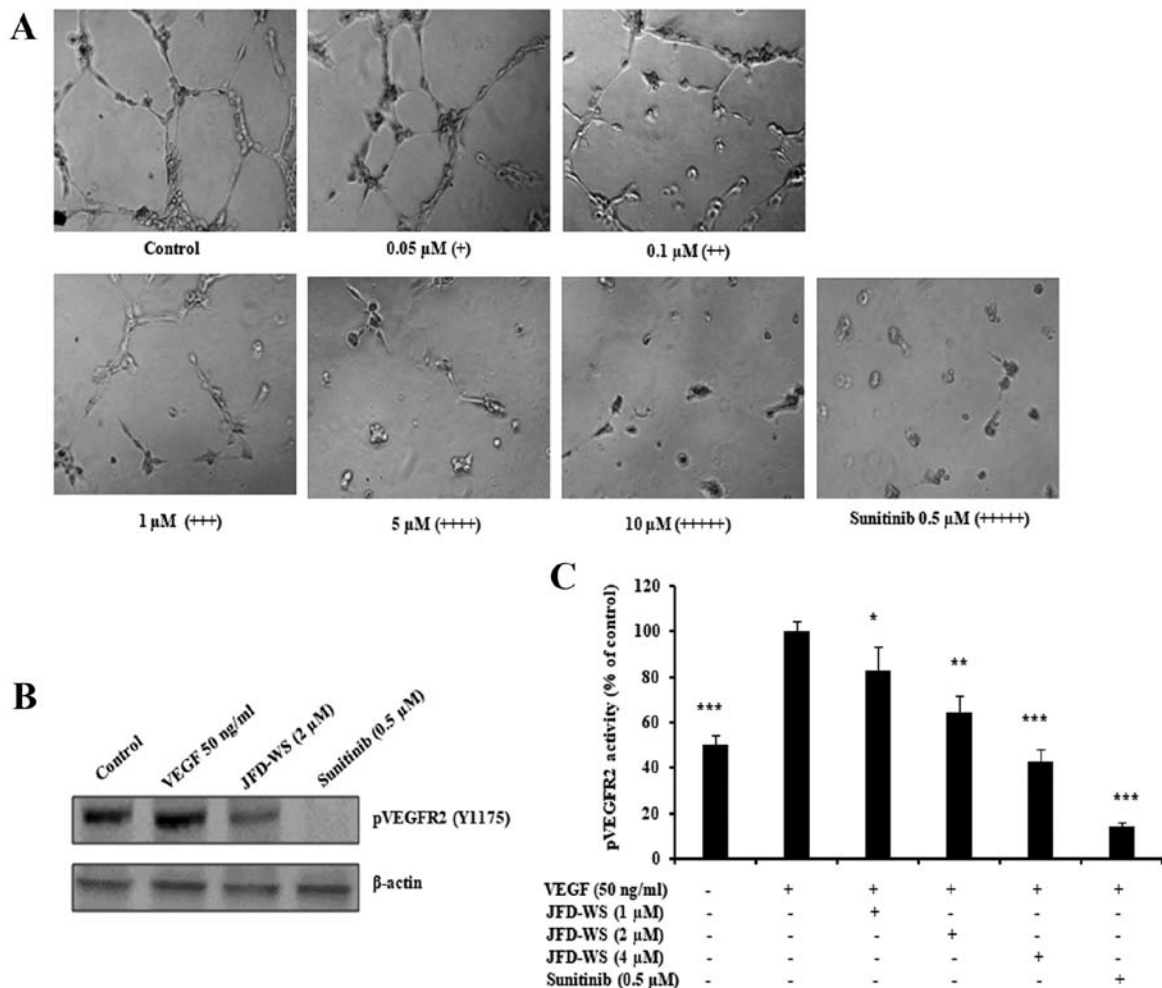


Figure 5. JFD-WS inhibits HUVEC tube formation. (A) HUVECs were seeded on a Matrigel layer and treated with different concentrations of JFD-WS (0.05-10 μ M). HUVEC tube formation was assessed 6 h later. The score is based on the extent of cellular networks: (++++), individual cells well separated; (+++), cells begin to migrate and align; (++) , cells lineup but do not sprout; (+), visible sprouting; and (+), closed polygons begin to form. (B) JFD-WS inhibited VEGF-induced phosphorylation of VEGFR2 in HUVECs. (C) The phosphorylation activity of VEGFR2 in the Tyr1175 phosphorylation site was measured after treatment with JFD-WS for 24 h using the PathScan Phospho-VEGFR2 Sandwich ELISA kit. The VEGF stimulated bar was compared with the basal level, which shows a significant elevation in the VEGFR2 phosphorylation. However, JFD-WS treatment showed a significant inhibition of pVEGFR2 levels caused by VEGF stimulation. Therefore, the VEGF stimulated effect was used as 100% for comparison. The error bar represents the SD for the results obtained from at least 3 independent experiments. Sunitinib (0.5 μ M) was used as a positive control (* P ≤0.05, ** P ≤0.01, *** P ≤0.005).

cell cycle controlling component p53, the effect of JFD-WS on the expression levels of p53 protein in the xenograft tumors was examined. A marked induction of p53 protein level (Fig. 9A) was observed in JFD-WS-treated tumors, nearing ~10-fold increase, while the p53 protein level in the combination treatment group was nearly 11-fold as compared with the control tumors (untreated). These results indicate that in addition to the anti-angiogenic effect, JFD-WS has the ability to induce apoptosis. The results also suggest that the induction of apoptosis in the xenografts may occur through induction of the intrinsic pathway consequent to the activation of p53-dependent pathways.

Effects of JFD-WS on Bcl-2 and Bax protein expression levels. Alteration in the levels of both Bcl-2 and Bax proteins have been shown to be associated with the anti- and pro-apoptotic functions, respectively. We explored the impact of JFD-WS treatment on the expression of Bcl-2 and Bax. As shown in Fig. 9A, JFD-WS monotherapy and also the combination

treatment decreased the Bcl-2 protein level significantly as compared to the levels of the control group. In addition, the expression level of Bax was increased by 4-fold in the group treated with JFD-WS alone. Likewise, in the JFD-WS/Taxol combination group, Bax level was increased by 5-fold as compared to the control.

Cytochrome c release and expression of APAF-1. The release of cytochrome c from mitochondria is critical for the initiation of APAF-1 mediated caspase activation which is shown to subsequently induce apoptosis in a multitude of experimental models. Therefore, we assessed the induction of cytochrome c release from mitochondria and the expression of APAF-1 in JFD-WS-treated and untreated groups. However, the increase in the cytochrome c level observed in the combination treatment group was only slightly higher when compared to treatment with JFD-WS alone. In consistent with these intracellular alterations, the immunoblotting analysis revealed a markedly increase in the expression of APAF-1 in both

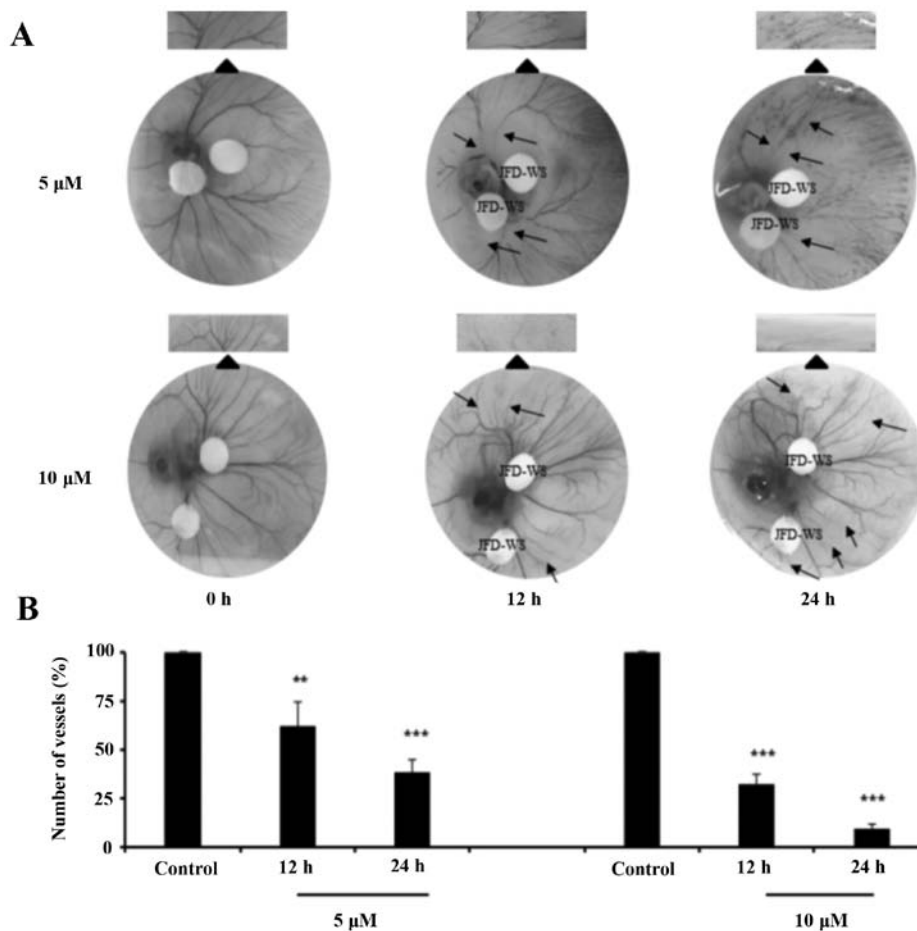


Figure 6. JFD-WS blocks angiogenesis. Four-day incubated fertilized chicken eggs were broken and the egg contents were transferred into sterile Petri dish. The vascular bed was incubated with 5 and 10 μM JFD-WS on both the sterile paper disc for 12 h. (A) The representative images confirm the inhibition of blood vessel formation in 5 and 10 μM JFD-WS. (B) Quantification of a number of branching blood vessels in the experiment groups with respect to the control (** $P \leq 0.01$, *** $P \leq 0.005$).

JFD-WS and combination treated groups as compared with the control (Fig. 9A).

Activation of caspase-3, PARP cleavage, and DNA fragmentation. Accumulated evidence from the literature indicates that caspases play a pivotal role in the terminal, execution phase of apoptosis (17). It is known that the activated caspase-3 receives apoptotic signals from mitochondria and transmits to PARP to act at the DNA level. To ascertain whether caspase-3 and PARP are involved in JFD-WS-induced cell death, the expression levels of active caspase-3 and PARP cleavage were examined. As shown in Fig. 9A, JFD-WS treatment alone was able to cause a significant increase in cleaved caspase-3 levels in the xenograft tumor leading to cleavage of PARP (Fig. 9A), which further evidenced the induction of apoptosis in the xenograft tumors subsequent to the anti-angiogenic effects elicited by JFD-WS. To confirm the final execution of apoptosis, the genomic DNA was isolated from tumors of the control and treated animals to determine DNA fragmentation. Electrophoretic separation of the genomic DNA revealed the fragmentation of DNA in the xenograft tumor tissues treated with JFD-WS as well as the JFD-WS+Taxol combination (Fig. 9B).

Safety profile of JFD-WS. Treatment of BALB/c mice with JFD-WS for 30 days did not cause any adverse effects as

revealed by the analysis of pathological and hematological parameters. Furthermore, no abnormal clinical signs or behavior were detected in either of the groups. Hematological observations of all treated mice, including total blood count, red blood cells (RBC), white blood cells (WBC), neutrophils, monocytes, lymphocytes, platelet counts and hemoglobin levels were within normal limits as the control group. There were no significant differences noted between control and treated groups for the hematological parameters measured (Table I). Conversely, it can be interpreted that the injection of JFD-WS at a dose of 100 mg/kg neither showed significant changes in serum biochemical parameters such as albumin, total protein, globulin, urea, sodium and creatinine levels when compared to control group nor revealed an abnormality in the functions of the vital organs (Table II). However, significant difference in the total bilirubin was observed in the Taxol and JFD+Taxol combination groups when compared with the control (Table II). Consistent with biomarker analyses, there were no observable changes in body weight, food intake, behavior and lethargy and gastrointestinal toxicity, in the combination treatment.

Pharmacokinetics of JFD-WS in mice. As mentioned previously, original JFD was modified into JFD-WS to increase its bioavailability. To test this, we investigated the pharmacokinetic (PK) profile of JFD-WS in BALB/c

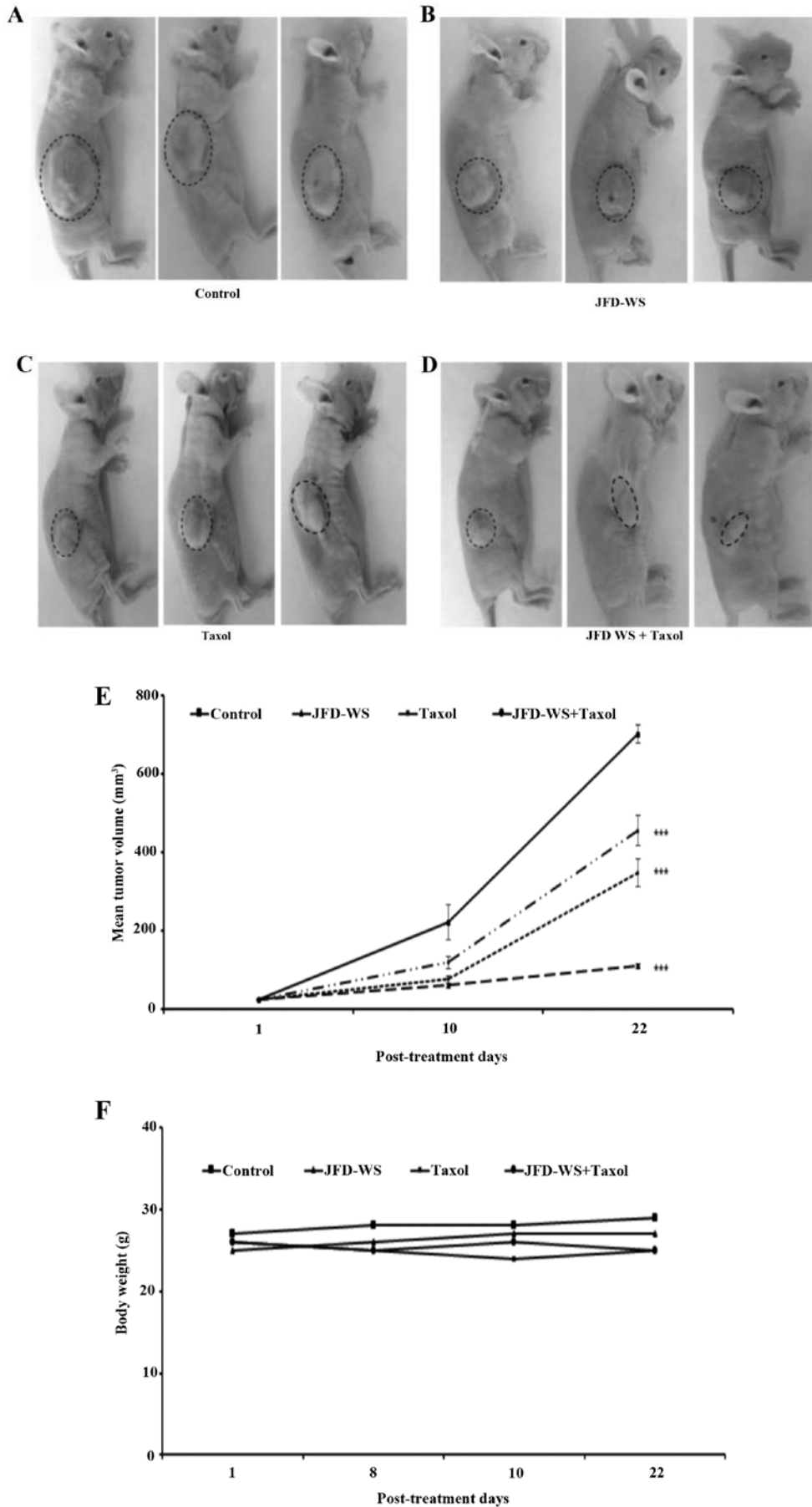


Figure 7. Effects of JFD-WS and Taxol combination on tumor growth in GI-101A breast adenocarcinoma xenograft mouse model. (A) Control. (B) JFD-WS (100 mg/kg). (C) Taxol (10 mg/kg) and (D) JFD-WS (100 mg/kg)+Taxol (10 mg/kg). (E) Changes in tumor volume. (F) Total body weight of xenograft mice after post tumor implantation (***P*≤0.005).

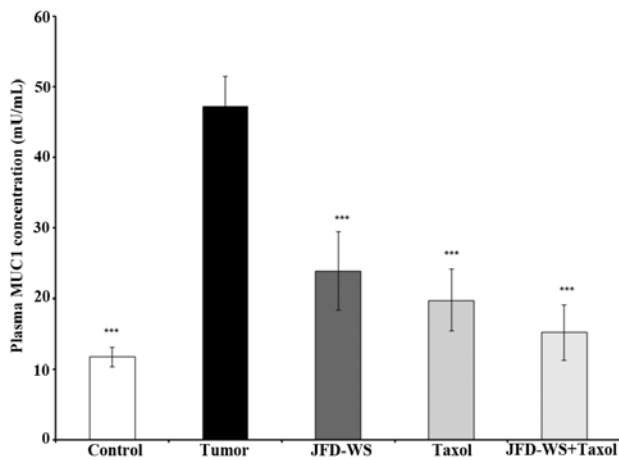


Figure 8. Concentrations of circulating MUC1 in the plasma of control and experimental groups. The plasma MUC1 level was measured after treatment with JFD-WS, Taxol and JFD-WS + Taxol combination using ELISA kit. Tumor burdened animals showed a significant elevation in plasma MUC1 levels when compared to the control (no tumor burden). In contrast, animals treated with JFD-WS, Taxol and combination showed a significant decrease in the levels of MUC-1 when compared to the tumor-bearing animals (** $P \leq 0.005$).

mice (Table III). The plasma profile was established by measuring the plasma concentrations of JFD-WS at different time points after i.p. administration of the drugs at the dose of 100 mg/kg body weight (Fig. 10A). JFD-WS reached a maximum plasma concentration after 15 min of i.p. administration when compared to oral administration (data not shown). Since JFD-WS is highly water soluble,

urine elimination was expected to be the major route of elimination. As expected, JFD-WS reached maximum urine elimination after 30 min of i.p. injection (Fig. 10B). Following i.p. injection, JFD-WS is largely distributed in extravascular regions as indicated by its volume of distribution. The results of PK studies confirm that i.p. administration allows for quick distribution of JFD-WS to tumor sites while high clearance rate could contribute to the lower toxicity of this compound.

Discussion

Overexpression and aberrant activation of receptor tyrosine kinases (RTKs) such as EGFR and VEGFR are associated with increased proliferation rates, angiogenesis and metastasis and reduced apoptosis (18). Our group has been engaged in the design, screening and testing for novel VEGFR2 inhibitors such as JFD (5,6). This molecule belongs to a class of organic compound which is analogous to the purine moiety (7-[2-hydroxy-3-(4-methoxyanilino)propyl]-1,3-dimethyl-3,7-dihydro-1H-purine-2,6-dione). The original form of JFD was modified to its water soluble form to increase bioavailability while preserving its pharmacological activities. Various studies directed towards the development of anti-angiogenic agents have used HUVECs as the cell based model to study physiological and pathological processes of angiogenesis (7). In addition, it provides an optimal model system for the study of the regulation of endothelial cells and their response to anti-angiogenic molecules (7). Recent results from our laboratory confirm the anti-angiogenic activity of JFD-WS by decreasing the level of VEGFR2 phosphorylation in human endothelial

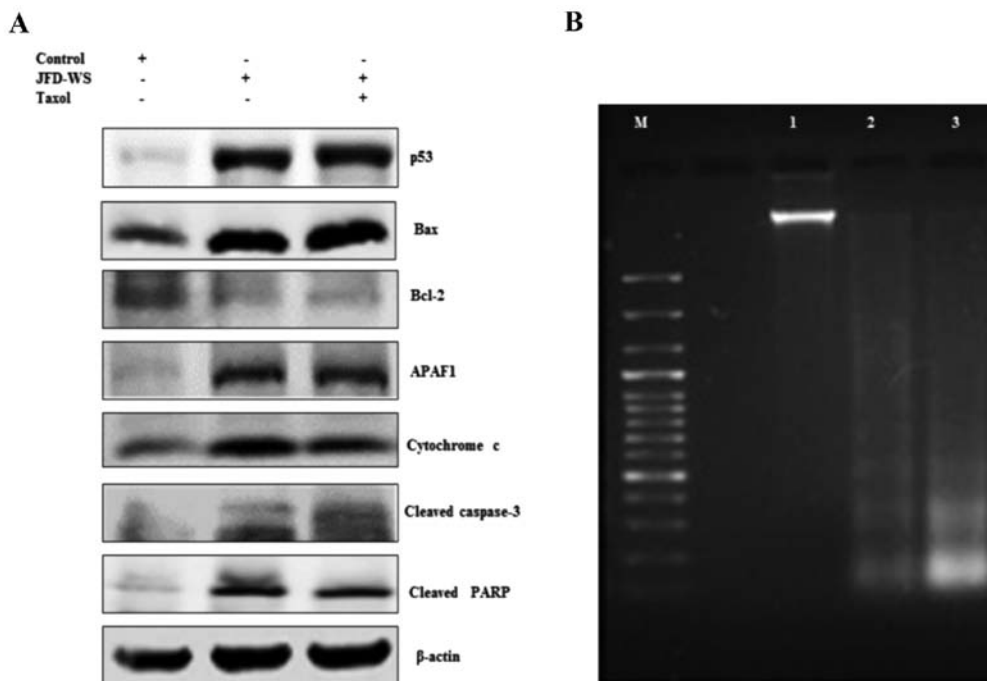


Figure 9. JFD-WS alters apoptotic signals in the xenograft tumors. (A) Expression of p53, Bax, Bcl-2, APAF-1, cytochrome *c*, cleaved caspase-3 and cleaved PARP proteins extracted from tumors of untreated control and treated groups were analyzed by western blotting. The protein extracts (25 μ g of protein) were separated by SDS-PAGE gel (7.5-12%). After electro-blotting, the separated proteins were probed with the corresponding antibody. Significant alteration in the expression pattern of pro- and anti-apoptotic proteins was observed in treatment groups as compared to untreated control tumor. β -actin was used as a loading control. (B) Demonstration of apoptosis by DNA fragmentation. Lane M, 100 bp DNA ladder; lane 1, DNA extracted from control tumors; lane 2, DNA extracted from JFD-WS-treated tumors and lane 3, DNA extracted from JFD-WS + Taxol-treated tumors. The DNA was separated by electrophoresis using 1.5% agarose gel and visualized using UVP image analyzer.

Table I. Hematological parameters after 30 days treatment with JFD-WS.

Parameters	Control	JFD-WS	Taxol	JFD-WS + Taxol
Red blood cell count	9.54±0.58	9.60±0.47	9.91±0.34	9.14±1.20
White blood cell count	3.07±0.65	3.87±1.6	3.57±0.20	5.47±0.55 ^a
Hemoglobin	13.17±0.29	13.33±0.40	12.13±0.81	12±1.90
Hematocrit	44.67±2.08	45±2.65	44±4.58	40±8
MCV	46.67±2.52	47±2	48±3.61	43.7±3.51
MCH	13.67±1.15	14±0	13.33±0.58	13±0
MCHC	29.67±0.58	29.33±1.15	27.33±2.08	30±1
Segmented neutrophils	0.53±0.15	0.49±0.41	1.2±0.77	1.08±0.26 ^a
Lymphocytes	2.15±0.51	1.83±0.41	2.31±0.31	2.92±0.73
Monocytes	0.17±0.03	0.17±0.01	0.14±0.04	0.20±0.05
Eosinophils	0.15±0.01	0.16±0.05	0.16±0.04	0.19±0.09
Basophils	0.06±0.01	0.05±0.02	0.07±0.01	0.07±0.03
RBC morphology	Normal	Normal	Normal	Normal
Platelet morphology	Normal	Normal	Normal	Normal
WBC morphology	Normal	Normal	Normal	Normal

MCV, mean corpuscular volume; MCH, mean corpuscular hemoglobin. Values are expressed as mean ± SD (^aP≤0.05).

Table II. Blood clinical chemistry values after administration of JFD-WS on BALB/c mice.

Parameters	Control	JFD-WS	Taxol	JFD-WS + Taxol
Glucose	111.70±22.3	106.30±12.70	106.70±20.20	98.3±10.20
BUN	21±2.65	15±1	20.33±1.15	19.70±2.89
CREA	0.20±0.00	0.20±0.00	0.17±0.06	0.20±0.00
BUN/crea ratio	105±13.20	75±5	106±15.70	98.3±14.4
Amylase	2799±513	2930±523	2529±78.6	2416±311
Calcium	7.93±0.37	8.60±0.00	8.77±0.38	7.90±2.25
Phosphorus	9.9±0.69	9.63±3.47	7.6±1.31	6.65±0.21
Total protein	6.17±0.21	5.57±0.40	5.33±1.31	5.77±0.40
Albumin	3.57±0.06	3.23±0.25	2.90±0.20	3.30±0.17
AST	294±53.80	251±69.70	281±65.80	319±87
ALT	54.67±8.08	55.67±13.10	79.67±39.30	89.30±25.70
CPK	2429±483	2403±554	2756±675	2281±765
Total bilirubin	0.77±0.15	0.52±0.08	0.33±0.12 ^a	0.47±0.21 ^a

BUN, blood urea nitrogen; CREA, creatinine; AST, aspartate transaminase; ALT, alanine transaminase; CPK, creatine phosphokinase. Values are expressed as mean ± SD (^aP≤0.05).

cells, through specific binding to VEGFR2 (19). As a result of VEGFR2 antagonism, JFD-WS specifically inhibits angiogenesis and some of the related events that include endothelial cell proliferation, migration, survival and vascular network formation (16). Conversely, when we extended these analyses to the *in vivo* systems, our results showed that new blood vessel formation on the CAM was significantly inhibited by JFD-WS even at sub-lethal concentrations, providing critical evidence to the ability of JFD-WS to inhibit angiogenesis.

Since many of the anti-angiogenic agents produce cytostatic effects (20), we evaluated the effects of JFD-WS alone

and also in combination with Taxol on GI-101A xenograft tumor implanted athymic nude mice. As outlined in the results section, beside the anti-angiogenic effect *in vitro*, JFD-WS also exerted cytoreductive activity on GI-101A xenograft implanted animals which were confirmed by the reduction in tumor volume (Fig. 7E). The mechanism of action of JFD-WS is similar to various anti-angiogenic inhibitors, which are known to inhibit tumor growth by blocking angiogenesis in the xenograft tumors (19). Inhibition of tumor growth under *in vivo* condition can be attributed primarily to the anti-angiogenic activity of JFD-WS. However, JFD-WS shows

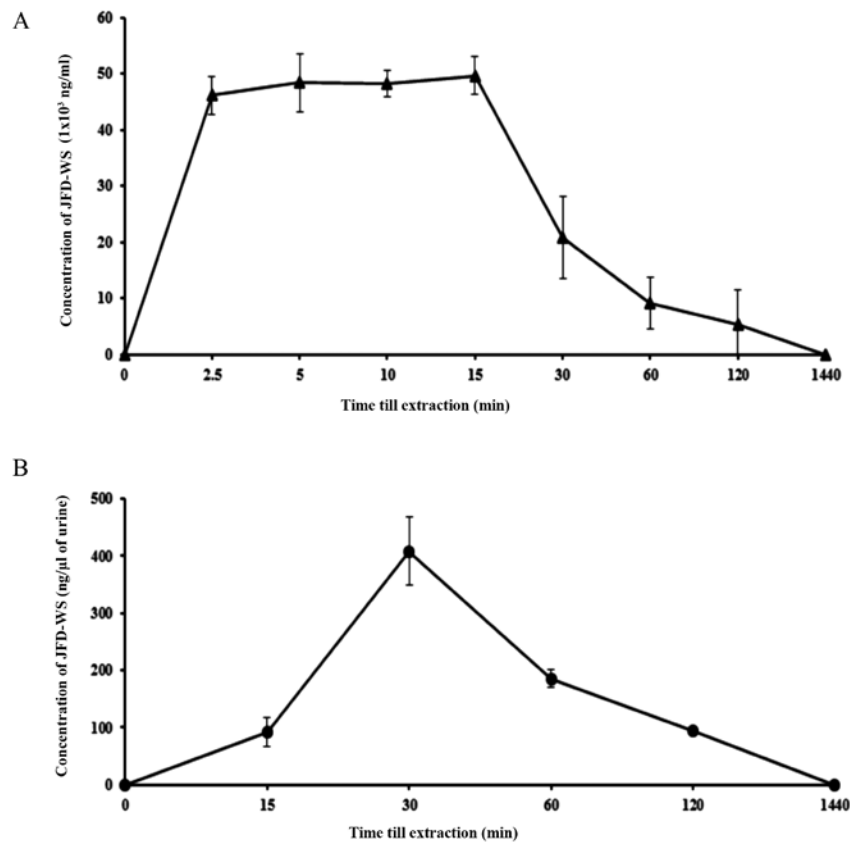


Figure 10. Concentration of JFD-WS in the biological samples. (A) Concentration of JFD-WS as calculated for 1 ml blood. (B) Concentration of JFD-WS in 1 µl urine.

Table III. Summary of pharmacokinetic parameters.

Pharmacokinetic parameters	JFD-WS (100 mg/kg body weight)
C_{max}	49.69 µg/ml
$T_{1/2}$	34 min
K_e	1.24 h ⁻¹
Vd	0.25 l
Cl	0.084 l/h

C_{max} , maximum concentration; $T_{1/2}$, elimination half-life; k_e , elimination rate constant; Vd, volume of distribution and Cl, clearance rate.

direct antiproliferative effects also on MCF-7 and GI-101A cells. Therefore, we are suspecting that combination of both these effects may contribute to the tumor-suppressing ability of JFD-WS. Induction of apoptosis is a therapeutic approach that is primarily intended to impede rapid tumor growth. With this purpose in the forefront, some of the earlier studies have shown that several VEGFR2 inhibitors including sorafenib can induce apoptosis in the HUVECs (21). However, in our experiments, subsequent to the onset of anti-angiogenic effect by JFD-WS, there appears to be the induction of apoptosis in the PDX tumors, which was confirmed by DNA fragmentation. Treatment with JFD-WS, both as a single agent and also in combination with Taxol, increased the expression of tumor

suppressor protein p53 in the xenograft tumors with a subsequent increase in the pro-apoptotic protein Bax. The increase in Bax levels was accompanied by significant decrease in the levels of the anti-apoptotic protein Bcl-2. In addition to the increase in the expression of Bax protein levels, a significant increase in the level of APAF-1 with a concomitant increase in the cytochrome *c* level was observed in the tumor samples of JFD-WS-treated animals as compared to the untreated controls, evidencing the activation of the apoptotic pathway.

In response to activation of apoptotic signals, cytochrome *c* is released from mitochondria to the cytosol, and it eventually binds to APAF-1 to form a procaspase-9 activating heptameric protein known as apoptosomes. Such apoptosomes are required for the activation of caspase-9 through autocatalysis, which subsequently generates the caspase-3 from procaspase-3 (22). Activation of caspase-3 eventually triggers the caspase-activated DNase, which enters the nucleus and causes DNA cleavage that was clearly evidenced from the present study (Fig. 9A). Subsequently, the active caspase-3 cleaves the downstream substrate PARP which is responsible for the morphological and biochemical changes that constitute the final stages of apoptosis (23,24). PARP cleavage, which is indicated by the generation of an 85-kDa fragment, has been reported to disable/prevent the DNA repair process which eventually leads to cell death (25).

Several studies have shown active cell death due to apoptosis following anti-angiogenic therapy. However, the actual cause of apoptotic cell death subsequent to anti-angiogenic therapy remains as an area with the limited amount of

knowledge and understanding. Although, several possibilities can be considered including direct effects coming from anti-angiogenic agents, inhibition of VEGFR2 phosphorylation by a small molecule is reported to induce apoptosis by inhibiting the PI3K/AKT pathway (26). In addition, decreased phosphorylation of AKT was shown to increase the p53 expression level and trigger the intrinsic pathway of apoptosis (25). Experimental evidence also suggests that p53 can negatively regulate VEGF expression and may decrease angiogenesis and vessel permeability, thereby inducing and sustaining the dormancy of the experimental tumors in micro-metastasis stages by elevating the incidence of apoptosis in tumor cells (27,28). Results observed in the present study with increased expression of p53 (Fig. 9A) following drug treatment tilting the balance towards apoptosis, is in agreement with the study from Fontanini *et al* (29) who showed the similar influence of the p53 tumor-suppressor gene in non-small-cell lung carcinoma (NSCLC).

Inhibition of VEGF/VEGFR2 with an increase in the active caspase-9 and caspase-3-mediated apoptosis in haemangioma-derived endothelial cells (HaemEC) has been previously reported (30). The decreased expression of anti-apoptotic protein Bcl-2 seen in the tumor tissues (Fig. 9A) with the concomitant increase in Bax level can easily shift the balance towards programmed cell death. Our results are similar to the inhibition of Bcl-2 by small molecules or antisense oligonucleotides that led to multiple effects on the tumor, including strong anti-angiogenic effect as well as restoration of sensitivity to antineoplastic agents and thereby inducing apoptosis (31). Substantial alteration in the expression level of anti-apoptotic protein Bcl-2 in JFD-WS treated mice that coincided with the decreased tumor volume, is unique and confirms the ability for JFD-WS to induce cancer cell death through multiple mechanisms.

Typically anti-angiogenic action of VEGFR2 inhibitors has been shown to induce apoptotic cell death of endothelial cells (ECs) that are part of the tumor vasculature (18). The apoptotic cell death of the ECs was primarily responsible for the reduced density of the tumor and regression of tumor growth. However, the present study shows significant initiation of pro-apoptotic signals in JFD-WS-treated tumor xenografts. In addition, both the JFD-WS and Taxol as monotherapy and in combination showed a significant reduction in the plasma level of tumor biomarker MUC1 further indicating the reduction in the tumor burden of the experimental animals subsequent to JFD-WS treatments.

Preliminary pharmacokinetic studies in mice confirm that JFD-WS is largely distributed to extravascular regions within a shorter duration of time after i.p injection, which enables JFD-WS to control tumor growth. However, being target selective, high urine clearance rate of JFD-WS contributed to the lower toxicity of this compound. In addition, hematological and serum biochemistry analysis of the mice treated with JFD-WS revealed no pathological changes. However, some of the VEGFR2 inhibitors that are already in clinical use have been found to inflict significant toxicities in the gastrointestinal tract and liver after single doses of treatment (21). Although, the effective dose of JFD-WS required for inhibition of tumor growth is slightly higher, the excellent safety profile of JFD-WS indicates that it has the potential to

be a safer and effective anti-angiogenic drug. In conclusion, our anti-angiogenic drug JFD-WS, whether used as a single agent or in combination with Taxol produced strong antitumor effects by inducing apoptosis of cancer cells in GI-101A breast xenograft tumor implanted athymic nude mice. Elevating p53 levels and inducing apoptosis is a unique property, and typically not seen with other anti-angiogenic drugs. Therefore, our JFD-WS may be one of its type of anti-angiogenic inhibitors with dual abilities.

Acknowledgements

The authors would like to thank the Royal Dames of Cancer Research, Inc. (Ft. Lauderdale, FL, USA) for their financial support in conducting this research. The authors would also like to acknowledge the research grant from the Community Foundation of Broward, Ft. Lauderdale (Florida, USA) which partially supported the present study.

References

1. Folkman J: Role of angiogenesis in tumor growth and metastasis. *Semin Oncol* 29 (Suppl 16): 15-18, 2002.
2. Hanahan D and Weinberg RA: Hallmarks of cancer: The next generation. *Cell* 144: 646-674, 2011.
3. Ivy SP, Wick JY and Kaufman BM: An overview of small-molecule inhibitors of VEGFR signaling. *Nat Rev Clin Oncol* 6: 569-579, 2009.
4. Kamba T and McDonald DM: Mechanisms of adverse effects of anti-VEGF therapy for cancer. *Br J Cancer* 96: 1788-1795, 2007.
5. Sridhar J, Akula N, Sivanesan D, Narasimhan M, Rathinavelu A and Pattabiraman N: Identification of novel angiogenesis inhibitors. *Bioorg Med Chem Lett* 15: 4125-4129, 2005.
6. Dhandayuthapani S and Rathinavelu A: JFD, a novel small molecule for inhibiting vascular endothelial growth factor receptor-mediated angiogenesis. In: Proceedings of the 105th Annual Meeting of the American Association for Cancer Research; 2014 Apr 5-9; San Diego, CA Philadelphia (PA): AACR; *Cancer Res* 74 (Suppl 19): Abstract nr1021, 2014.
7. Auerbach R, Akhtar N, Lewis RL and Shinnars BL: Angiogenesis assays: Problems and pitfalls. *Cancer Metastasis Rev* 19: 167-172, 2000.
8. Mekhail TM and Markman M: Paclitaxel in cancer therapy. *Expert Opin Pharmacother* 3: 755-766, 2002.
9. Ramaswamy B and Puhalla S: Docetaxel: A tubulin-stabilizing agent approved for the management of several solid tumors. *Drugs Today* 42: 265-279, 2006.
10. Dorr RT: Pharmacology of the taxanes. *Pharmacotherapy* 17: 96S-104S, 1997.
11. Hollstein M, Hergenbahn M, Yang Q, Bartsch H, Wang ZQ and Hainaut P: New approaches to understanding p53 gene tumor mutation spectra. *Mutat Res* 431: 199-209, 1999.
12. Senapati S, Das S and Batra SK: Mucin-interacting proteins: From function to therapeutics. *Trends Biochem Sci* 35: 236-245, 2010.
13. Tampellini M, Berruti A, Gerbino A, Buniva T, Torta M, Gorzegno G, Faggiuolo R, Cannone R, Farris A, Destefanis M, *et al*: Relationship between CA 15-3 serum levels and disease extent in predicting overall survival of breast cancer patients with newly diagnosed metastatic disease. *Br J Cancer* 75: 698-702, 1997.
14. Morrissey JJ and Raney S: A metastatic breast tumor cell line, GI-101A, is estrogen receptor positive and responsive to estrogen but resistant to tamoxifen. *Cell Biol Int* 22: 413-419, 1998.
15. Tamilarasan KP, Kolluru GK, Rajaram M, Indhumathy M, Saranya R and Chatterjee S: Thalidomide attenuates nitric oxide mediated angiogenesis by blocking migration of endothelial cells. *BMC Cell Biol* 7: 17, 2006.
16. Lamalice L, Le Boeuf F and Huot J: Endothelial cell migration during angiogenesis. *Circ Res* 100: 782-794, 2007.
17. Budihardjo I, Oliver H, Lutter M, Luo X and Wang X: Biochemical pathways of caspase activation during apoptosis. *Annu Rev Cell Dev Biol* 15: 269-290, 1999.

18. Jimeno A and Hidalgo M: Pharmacogenomics of epidermal growth factor receptor (EGFR) tyrosine kinase inhibitors. *Biochim Biophys Acta* 1766: 217-229, 2006.
19. Kanagasabai T, Alvarez J, Bhalani M, Dhandayuthapani S and Rathinavelu A: The in vivo activity of a novel anti-angiogenic compound, JFD-WS, in human breast adenocarcinoma xenograft implanted athymic nude mice. In: Proceedings of the 106th Annual Meeting of the American Association for Cancer Research; 2015 Apr 18-22; Philadelphia (PA): AACR; *Cancer Res* 75 (Suppl 15): Abstract nr1380, 2015.
20. Gotink KJ and Verheul HM: Anti-angiogenic tyrosine kinase inhibitors: What is their mechanism of action? *Angiogenesis* 13: 1-14, 2010.
21. Yang F, Brown C, Buettner R, Hedvat M, Starr R, Scuto A, Schroeder A, Jensen M and Jove R: Sorafenib induces growth arrest and apoptosis of human glioblastoma cells through the dephosphorylation of signal transducers and activators of transcription 3. *Mol Cancer Ther* 9: 953-962, 2010.
22. Susin SA, Zamzami N, Castedo M, Daugas E, Wang HG, Geley S, Fassy F, Reed JC and Kroemer G: The central executioner of apoptosis: Multiple connections between protease activation and mitochondria in Fas/APO-1/CD95- and ceramide-induced apoptosis. *J Exp Med* 186: 25-37, 1997.
23. Zamzami N, Marchetti P, Castedo M, Zanin C, Vayssière JL, Petit PX and Kroemer G: Reduction in mitochondrial potential constitutes an early irreversible step of programmed lymphocyte death in vivo. *J Exp Med* 181: 1661-1672, 1995.
24. Marchetti P, Castedo M, Susin SA, Zamzami N, Hirsch T, Macho A, Haeflner A, Hirsch F, Geuskens M and Kroemer G: Mitochondrial permeability transition is a central coordinating event of apoptosis. *J Exp Med* 184: 1155-1160, 1996.
25. Kroemer G and Reed JC: Mitochondrial control of cell death. *Nat Med* 6: 513-519, 2000.
26. Gottlieb TM, Leal JF, Seger R, Taya Y and Oren M: Cross-talk between Akt, p53 and Mdm2: Possible implications for the regulation of apoptosis. *Oncogene* 21: 1299-1303, 2002.
27. Mukhopadhyay D, Tsiokas L and Sukhatme VP: Wild-type p53 and v-Src exert opposing influences on human vascular endothelial growth factor gene expression. *Cancer Res* 55: 6161-6165, 1995.
28. Bouvet M, Ellis LM, Nishizaki M, Fujiwara T, Liu W, Bucana CD, Fang B, Lee JJ and Roth JA: Adenovirus-mediated wild-type p53 gene transfer down-regulates vascular endothelial growth factor expression and inhibits angiogenesis in human colon cancer. *Cancer Res* 58: 2288-2292, 1998.
29. Fontanini G, Boldrini L, Vignati S, Chinè S, Basolo F, Silvestri V, Lucchi M, Mussi A, Angeletti CA and Bevilacqua G: Bcl2 and p53 regulate vascular endothelial growth factor (VEGF)-mediated angiogenesis in non-small cell lung carcinoma. *Eur J Cancer* 34: 718-723, 1998.
30. Kumar P, Miller AI and Polverini PJ: p38 MAPK mediates gamma-irradiation-induced endothelial cell apoptosis, and vascular endothelial growth factor protects endothelial cells through the phosphoinositide 3-kinase-Akt-Bcl-2 pathway. *J Biol Chem* 279: 43352-43360, 2004.
31. Milella M, Estrov Z, Kornblau SM, Carter BZ, Konopleva M, Tari A, Schober WD, Harris D, Leysath CE, Lopez-Berestein G, *et al*: Synergistic induction of apoptosis by simultaneous disruption of the Bcl-2 and MEK/MAPK pathways in acute myelogenous leukemia. *Blood* 99: 3461-3464, 2002.